

# DEPENDENCE OF MICROHARDNESS ON ANNEALING TIME OF AMORPHOUS Al-Mm-Ni-(Fe,Co) ALLOYS

H. Dimitrov, J. Latuch, G. Cieślak and T. Kulik

Faculty of Materials Science and Engineering, Warsaw University of Technology, Woloska 141, 02-507 Warsaw, Poland

Received: December 14, 2004

**Abstract.** Al-Mm-Ni-(Fe,Co) alloys of two slightly different compositions were melt spun to amorphous ribbons. DSC studies of the ribbons show that the first crystallization stage, responsible for the precipitation of fcc-Al, is well separated from the following. Mixed structures containing nanosized fcc-Al crystals, embedded in amorphous matrix were obtained by isothermal annealing of the initially amorphous ribbons for different times and thus, different crystalline fractions the fcc-Al crystals were obtained. The microhardness of the alloys increases with the increase of annealing time, reaching values of about 550 HV0.02 after 60 min of annealing. Replacing Fe by Co does not significantly influence the microhardness of these alloys. The slight changes of chemical composition do not seem to have a clear effect on microhardness.

## 1. INTRODUCTION

The nanocrystalline Al-based alloys have become very interesting, because of their excellent mechanical properties, compared to the commercial Al alloys. Tensile strength of about 1 GPa and 1.5 GPa have been reported for amorphous and nanocrystalline Al-based alloys, respectively [1]. Typically the rapidly quenched alloy is in the form of a thin ribbon.

The structure of the quaternary nanocrystalline Al-rare-earth (RE) – transition metal (TM) alloys consists of nanosized Al crystals, embedded in an amorphous matrix [2-4]. One way to obtain such structure is to anneal isothermally an amorphous Al alloy at temperatures below the onset crystallisation temperature of the alloy. The mechanical properties of these alloys increase with the increase of the crystalline fraction of the aluminium nanoparticles. As the rare-earth elements are very expensive, replacing them with mischmetal (Mm) reduces the cost of the material.

## 2. EXPERIMENTAL

Ingots of quaternary  $Al_{88}Mm_4Ni_5Fe_3$  and  $Al_{88}Mm_4Ni_5Co_3$  alloys were prepared from pure elements by arc melting in an argon atmosphere. Composition of mischmetal (Mm), in at.%, was: Ce-50.3, La-43.5, Pr-5.9, and Nd-0.3. During melt-spinning, the melt is ejected from a quartz crucible onto a copper wheel rotating at peripheral speed of 30-40  $ms^{-1}$ . The resulting ribbons were typically 2-3 mm wide and 30-40  $\mu m$  thick. In order to obtain nanocrystalline ribbon, pieces of the amorphous ribbons were vacuum-sealed in quartz crucibles and annealed at 492K in a laboratory tube furnace for 20 and 60 min. Differential scanning calorimetry (Perkin-Elmer DSC-7) was used to characterise the crystallisation process of the amorphous ribbons. The phase composition and average grain size were analysed by X-ray diffraction technique (XRD) using a Philips diffractometer operating with  $Cu K_{\alpha}$  radiation. The Vickers microhardness was measured using a Hanneman hardness tester with a load of 20 g. Microhardness was measured on the cross sec-

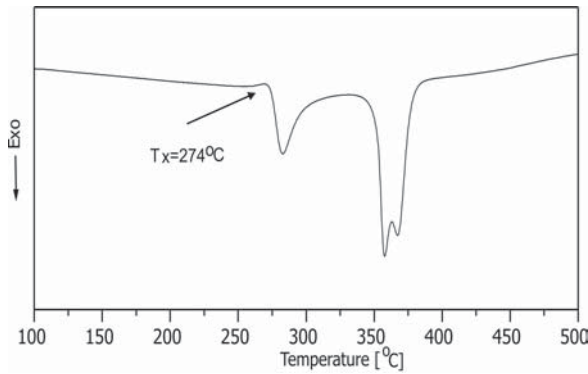


Fig. 1. DSC curve of  $\text{Al}_{88}\text{Mm}_4\text{Ni}_5\text{Fe}_3$  alloy.

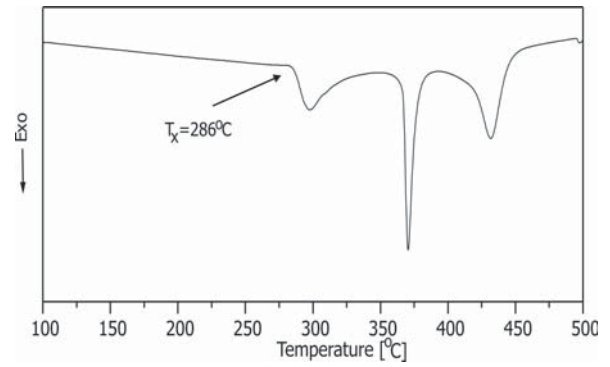


Fig. 2. DSC curve of  $\text{Al}_{88}\text{Mm}_4\text{Ni}_5\text{Co}_3$  alloy.

tion of the ribbons. To improve the statistics of the results, ten measurements were performed.

### 3. RESULTS

The DSC curves, taken at heating rate  $40 \text{ K min}^{-1}$ , are presented in Figs. 1 and 2. In both cases the crystallisation process occurs through more than one stage. As seen on the curves, the first crystallisation stage is characterised by a broad DSC peak, well separated from the second one. The absence of overlapping between the first and the second DSC peaks makes the process of crystallisation easier to perform and to control. Figs. 3 and 4 show the XRD patterns of the initial ribbons. A broad peak, typical for amorphous alloys, is seen for both compositions. The XRD patterns (Figs. 5-8) of both alloys after isothermal annealing for 20 and 60 minutes at temperatures below the crystallisation onset prove that the first DSC peak corresponds to

the precipitation of  $\alpha\text{-Al}$ . The average grain size, estimated by Scherrer formula from XRD patterns, was about 7-10 nm. It has been found that the particles size of the Al phase are nearly the same in all isothermally annealed samples.

The changes of the microhardness values with the increase of the annealing time are plotted in Fig. 9. It is seen that in both cases the increase of the annealing time leads to an increase of the microhardness values. This increase is very rapid for shorter annealing times and after about 20 minutes of annealing slightly 'flattens'. It means that the evolution of crystalline volume fraction between 20 and 60 min of annealing at 492K is very small. The increase of the microhardness with the annealing time is assumed to result from the increase of the crystalline fraction of the Al-particles.

Two different models have been developed to explain the relationship between hardness and microstructure of two-phase amorphous-crystalline Al-

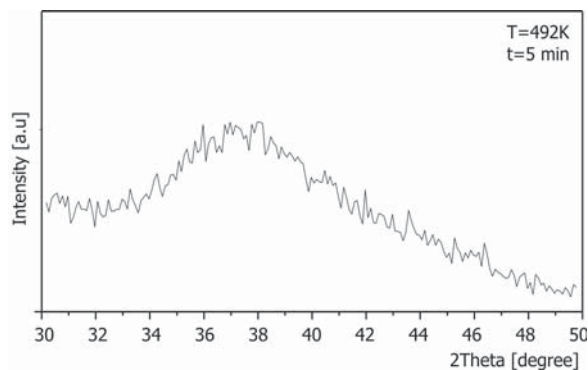


Fig. 3. X-Ray pattern of amorphous  $\text{Al}_{88}\text{Mm}_4\text{Ni}_5\text{Fe}_3$  alloy.

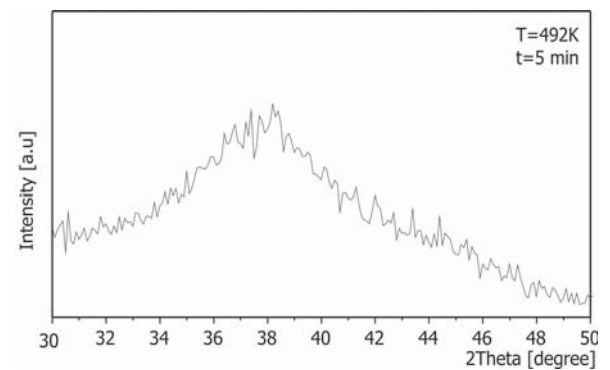
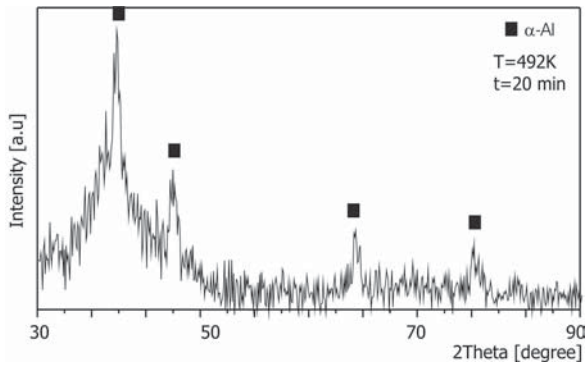
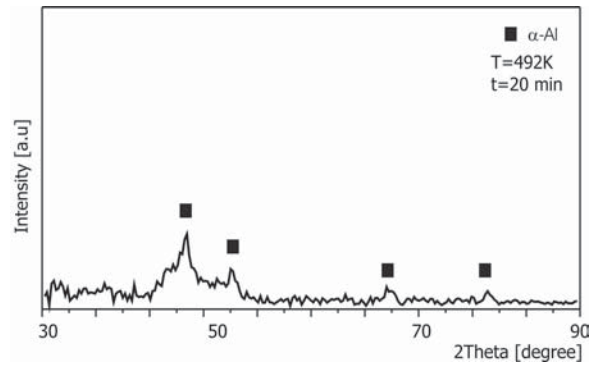


Fig. 4. X-Ray pattern of amorphous  $\text{Al}_{88}\text{Mm}_4\text{Ni}_5\text{Co}_3$  alloy.



**Fig. 5.** X-Ray pattern of  $\text{Al}_{88}\text{Mm}_4\text{Ni}_5\text{Fe}_3$  alloy after isothermal annealing at 492K for 20 min.



**Fig. 6.** X-Ray pattern of  $\text{Al}_{88}\text{Mm}_4\text{Ni}_5\text{Co}_3$  alloy after isothermal annealing at 492K for 20 min.

based materials. According to the first model, proposed by Zhong [5], the increase of hardness with crystalline volume fraction of  $\alpha$ -Al phase, is directly related to the hardening of the residual amorphous matrix because of its enrichment in elements different than Al (solute elements), due to the low solubility of these elements in the  $\alpha$ -Al phase, which can be considered close to pure Al [6].

The second model, developed by Kim [7], is known as the mixture model. Microhardness of the system is obtained as an average of the hardness of the residual amorphous matrix and the hardness of the defect-free, and therefore very hard,  $\alpha$ -Al crystals. The average is weighted using their respective volume fractions.

Therefore, it is hard to distinguish between the predictions of both models if absolute values of crystalline volume fraction are not obtained. In our case, measurement of the microhardness of crystalline ribbons leads to a value of 550 HV0.02, which is similar to the values reported for nanocrystalline Al-Y-Ni [5] ribbons.

#### 4. CONCLUSIONS

1. Isothermal annealing of amorphous  $\text{Al}_{88}\text{Mm}_4\text{Ni}_5(\text{Fe},\text{Co})_3$  alloys at temperatures below the temperatures of the crystallisation onset leads to the formation of structures, consisting of nanosized (7-10nm) Al crystals embedded in the amorphous matrix.
2. The microhardness of the alloys studied increases from about 300 up to about 550 with the increase of the annealing time from 2 to 60 min.
3. The increase of the annealing time from 2 to 60 min results in higher fraction of the crystallised Al-phase of the nanocrystalline alloys.

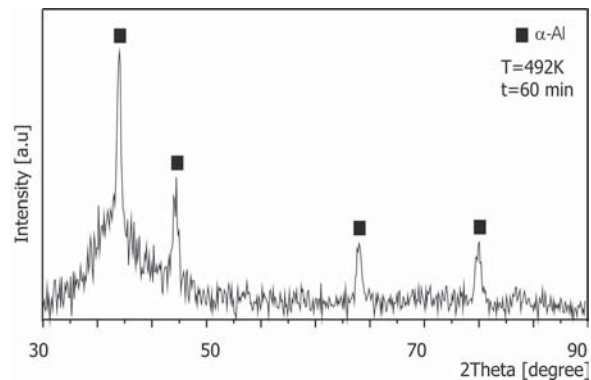


**Fig. 7.** X-Ray pattern of  $\text{Al}_{88}\text{Mm}_4\text{Ni}_5\text{Fe}_3$  alloy after isothermal annealing at 492K for 60 min.

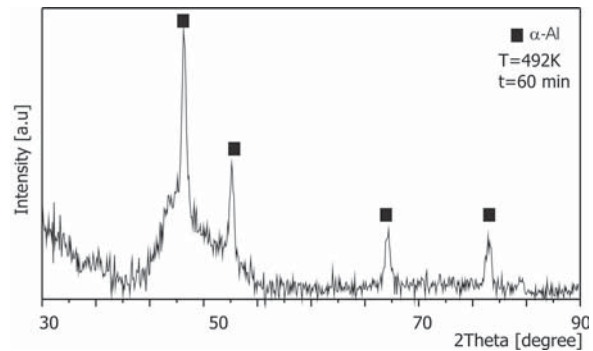


**Fig. 8.** X-Ray pattern of  $\text{Al}_{88}\text{Mm}_4\text{Ni}_5\text{Co}_3$  alloy after isothermal annealing at 492K for 60 min.

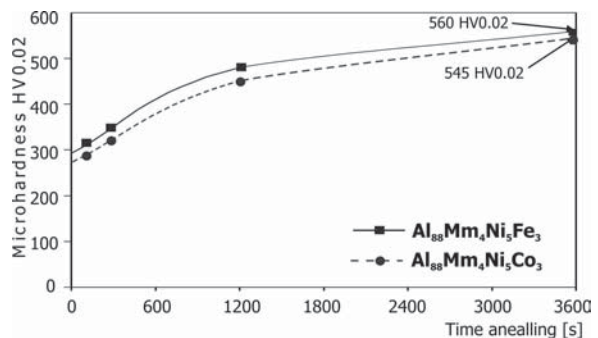


**Fig. 9.** Dependence of the microhardness on the annealing time of nanocrystalline  $\text{Al}_{88}\text{Mm}_4\text{Ni}_5(\text{Co}, \text{Fe})_3$  alloys.

4. Replacing Fe by Co does not change significantly the microhardness of the nanocrystalline Al-based alloys.

## REFERENCES

- [1] A. Inoue, K. Othara, A.P. Tsai and T. Masumoto // *J. Jpn. Appl. Phys.* **27** (1998) L280.
- [2] Y.H. Kim, A. Inoue and T. Masumoto // *Mater. Trans. JIM* **31** (1990) 747.
- [3] A. Inoue, Y.H. Kim and T. Masumoto // *Mater. Trans. JIM* **33** (1992) 487.
- [4] J. Latuch, T. Kulik and H. Dimitrov // *Mater. Sci. Eng.* **A 375-377** (2004) 956.
- [5] Z.C. Zhong, X.Y. Jiang and A.L. Greer // *Mater. Sci. Eng.* **A 226-228** (1997) 531.
- [6] K. Hono, Y. Zhang, A.P. Tsai, A. Inoue and T. Sakurai // *Scripta Metall* **32** (1995) 191.
- [7] H.S. Kim, P.J. Warren, B. Cantor and H.R. Lee // *NanoStructured Mater* **11** (1999) 241.